

See discussions, stats, and author profiles for this publication at: <https://www.researchgate.net/publication/325629356>

A Modified Uniaxial Bouc–Wen Model for the Simulation of Transverse Lateral Pipe–Cohesionless Soil Interaction

Conference Paper · June 2018

DOI: 10.1061/9780784481479.003

CITATION

1

READS

148

2 authors:



Kien Nguyen

California Institute of Technology

2 PUBLICATIONS 1 CITATION

[SEE PROFILE](#)



Domniki Asimaki

California Institute of Technology

116 PUBLICATIONS 1,471 CITATIONS

[SEE PROFILE](#)

Some of the authors of this publication are also working on these related projects:



Reduced-order models for dynamic soil-structure interaction analyses of buried structures [View project](#)



Seismic Safety and Resilience of Schools in Nepal [View project](#)

A modified uniaxial Bouc-Wen model for the simulation of transverse lateral pipe-cohesionless soil interaction

(FINAL DRAFT)

Kien T. Nguyen, S.M.ASCE¹ and Domniki Asimaki, Sc.D²

¹Department of Mechanical and Civil Engineering, California Institute of Technology, Pasadena, CA 91125; e-mail: ktnguyen@caltech.edu

²Department of Mechanical and Civil Engineering, California Institute of Technology, Pasadena, CA 91125; e-mail: domniki@caltech.edu

DOI: <https://doi.org/10.1061/9780784481479.003>

ABSTRACT

This paper proposes a modified uniaxial Bouc-Wen model to evaluate reaction force-displacement backbone curve for transverse lateral pipe-cohesionless soil interaction. The model is capable of representing the nonlinearity and the smooth transition zone of the curve. Using Unscented Kalman filter, the model parameter κ that controls the smoothness of transition zone is derived, on the basis of results from high-fidelity validated finite element analyses. κ is larger in loose sand compared to that in dense sand, implying a smoother transition zone of the curve for loose sand. There is a slight change of κ with pipe burial depth in case of dense sand, while the change is clearer and larger in loose sand. The variation of κ is related to the "passive-wedge" and "plow-through" failure mode of soil. The model is subsequently implemented in a series of soil-pipe interaction configurations, and the reaction force-deformation curves are found in good agreement with experimental data.

INTRODUCTION

Pipelines are one of the most important civil systems, conveying water, gas from production fields to residential and industrial areas. Most of the pipelines are buried underground and can be severely affected by geohazards such as earthquakes, landslides, and fault movements (O'Rourke, 2010). Therefore, it is vital to understand the interaction between the pipe and surrounding soil. Analytical models have been developed on the basis of soil subgrade reaction to analyze this problem. The surrounding soil is modeled as a series of independent, discrete springs with different stiffness whereas pipe is modeled as a structural beam/shell element. The accuracy of this model primarily depends on the mechanical parameters of structural elements used to represent pipe and soil. The current practices use elasto-plastic and nonlinear load-deformation characteristics for soil springs, as in the guidelines of ASCE (1984); ALA (2005); PRCI (2009). Since even in monotonically loading test, the behavior of the system is nonlinear from the beginning (Prisco, 2012), the nonlinear characteristic is preferable to achieve more accurate results. Jung et al. (2016) described a rectangular hyperbola representation of the reaction-displacement curves for cases of monotonically uniaxial loading tests. This paper develops a new versatile physical-based

methodology, originated from Bouc-Wen (BW) model that is capable of representing a wide range of nonlinearity of the backbone curves. It is also potentially extended to capture the mutual interaction between soil springs in different directions (coupled behavior) and the irreversible displacement of the soil in cyclic/dynamic problems.

This paper is divided into four sections. The first section presents the modified Bouc-Wen (MBW) model and its key input parameters. The second section describes the numerical finite element simulation used to generate the reaction-displacement curves. From those curves, the procedure of estimating κ for loose and dense sand via Unscented Kalman filter (UKF) is described in the third section. In the fourth section, the MBW method is compared with original BW method, elasto-plastic method and three different existing experiments.

MODIFIED UNIAXIAL BOUC-WEN MODEL

From the model originated by Bouc (1971) and subsequently extended by Wen (1976), the transverse lateral soil reaction force F per unit length of pipe can be expressed by

$$F = \alpha K u + (1 - \alpha) F_u \zeta \quad (1)$$

where: α is the ratio between post-yield stiffness and initial stiffness of the soil, K is the soil initial stiffness, u is the relative lateral displacement between the pipe and soil, F_u is the ultimate soil reaction force (yield strength), ζ is the dimensionless hysteresis parameter. ζ controls the nonlinearity of the reaction force-displacement curve. It is governed by

$$\dot{\zeta} = \frac{1}{u_0} (1 - |\zeta|^n (\beta \text{sign}(\dot{u}\zeta) + \gamma)) \dot{u} \quad (2)$$

where: $u_0 = F_u/K$ is the yield displacement, β and γ control the unloading-reloading stiffness ($\beta + \gamma = 1$), n controls the smoothness of the curve. This has been employed successfully to simulate the interaction between structures (pile, caisson foundation) and cohesionless soil (Badoni and Makris, 1996; Gerolymos and Gazetas, 2006; Varun and Assimaki, 2012; Varun et al., 2013).

However, the equation (2) only captures a limited range of nonlinear backbone curves (shaded area between 2 curves $n=1$ and $n=+\infty$ in Fig. 1). For the pipe-soil interaction problems, the backbone curves are likely to be outside of the aforementioned area, especially for the cases of loose sand. To overcome that, the function $|\zeta|^n$ can be replaced by any monotonically increasing function $f(\zeta)$ in the domain $[0, 1]$ with $f(0) = 0$ and $f(1) = 1$. This paper employed the normalized function $\tanh(\kappa|\zeta|) / \tanh \kappa$, which was originally used by Varun and Assimaki (2012); Varun et al. (2013) for pile foundation. The equation is written as

$$\dot{\zeta} = \frac{1}{u_0} \left(1 - \frac{\tanh(\kappa|\zeta|)}{\tanh \kappa} (\beta \text{sign}(\dot{u}\zeta) + \gamma) \right) \dot{u} \quad (3)$$

Badoni and Makris (1996); Ma et al. (2004) pointed out that (β, γ) parameters have minor significance. Therefore, they are taken as constants (0.5, 0.5) in this paper. Also, $\alpha = 0$, which indicates the soil post-yield stiffness is zero, is appropriate for representing plastic soil behavior.

Three parameters F_u , K , κ significantly affect the backbone curve $F - u$. The ultimate soil reaction F_u which can be found from many guidelines (ASCE, 1984; ALA, 2005; PRCI, 2009) is

not repeated here. Besides, on the basis of experimental and numerical results, Audibert and Nyman (1977); Trautmann and O'Rourke (1985); Jung et al. (2016) showed that the $F - u$ relationship can be represented by a hyperbolic curve of the form $F = \frac{u}{A' + B'u}$. From that, the initial soil stiffness can be calculated by

$$K = \left. \frac{\partial F}{\partial u} \right|_{u \rightarrow 0} = \frac{1}{A'} \quad (4)$$

The parameter κ plays a role similar to n in the original BW model, controlling the smoothness of the transition zone of the backbone curve, as illustrated in Fig. 1. The procedure for determining κ is the main focus of this paper and is presented in the subsequent sections.

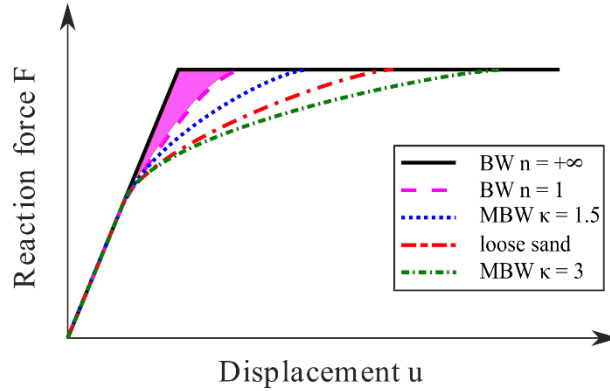


Figure 1. Smoothness of the transition zones depending on n (BW) and κ (MBW)

NUMERICAL SIMULATION

Finite Element model. Finite Element (FE) analyses were carried out to generate backbone curves $F - u$ for loose and dense sand, which will be used subsequently for estimating κ . The FE analyses of the interaction between pipe and sand were conducted using Ls-Dyna solver. In the model, constant stress hexahedron elements with hourglass control were used to simulate the soil medium. The pipe was modeled as a rigid cylinder. To ensure the plane strain condition, all nodes were constrained in the out-of-plane direction. Fig. 2 shows the mesh for simulating lateral soil-pipe interaction. In soils exhibiting softening behavior, strain localization and shear band formation typically result in mesh distortion (Mitchell and Soga, 2005). For that reason, near the pipe, the mesh was denser with smaller soil elements to increase the accuracy of the simulation. Nodes at two sides were constrained in horizontal direction while nodes at the bottom were fixed in both horizontal and vertical directions. The numerical simulation was executed in two stages. An initial geostatic loading was applied to soil and pipe to generate balanced stress state in the soil medium. During the subsequent quasi-static stage, lateral pipe movement was imposed by applying slow displacement to all pipe nodes. To increase the stability of the simulation, a small value of cohesion $c = 0.1$ kPa was used. Simulations were run with different values of cohesion (from 0 to 0.1 kPa) to prove that this small value has negligible effect on the results. The pipe-soil interaction interface was modeled by the Automatic-Nodes-To-Surface contact type (Hallquist et al., 2016). The pipe-soil friction angle was taken as 60% of soil friction angle (Trautmann and O'Rourke, 1985).

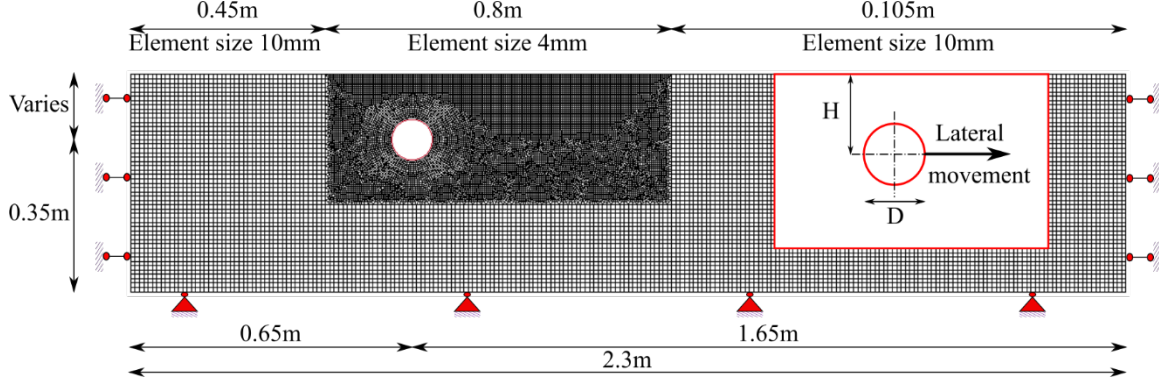


Figure 2. Geometry of the numerical model

Constitutive model for soil. Soil behavior was simulated by elastic-perfectly plastic model with Morh-Coulomb (MC) yield surface and non-associated flow rule. In MC model, the strength of soil is typically represented by two features: peak plane strain internal friction angle φ'_{ps-p} and peak dilation angle ψ_p . For dense sand, the mobilized friction angle φ'_{mob} and mobilized dilation angle ψ_{mob} are φ'_{ps-p} and ψ_p , respectively, where plastic shear strain $\gamma^p = 0$. They decrease to critical values φ'_{crit} and 0 as γ^p increases to illustrate the strain-softening (post-peak) behavior of dense sand. Anastasopoulos et al. (2007) and Jung et al. (2013) assumed a linear variation of friction and dilation angle with γ^p . In this paper, a similar approach is employed, except that the transition zone from the peak to critical value is expressed by a smooth symmetric beta distribution density function

$$\psi_{mob} = \begin{cases} 4^\alpha \left(\left(\frac{1}{2} - \frac{\gamma^p}{\gamma_c^p} \right) \left(\frac{1}{2} + \frac{\gamma^p}{\gamma_c^p} \right) \right)^\alpha \psi_p & \text{if } \gamma^p \leq \gamma_c^p \\ 0 & \text{if } \gamma^p > \gamma_c^p \end{cases} \quad (5)$$

$$\varphi'_{mob} = \begin{cases} \varphi'_{crit} + 4^\alpha \left(\left(\frac{1}{2} - \frac{\gamma^p}{\gamma_c^p} \right) \left(\frac{1}{2} + \frac{\gamma^p}{\gamma_c^p} \right) \right)^\alpha (\varphi'_{ps-p} - \varphi'_{crit}) & \text{if } \gamma^p \leq \gamma_c^p \\ \varphi'_{crit} & \text{if } \gamma^p > \gamma_c^p \end{cases}$$

where α is a parameter controlling the sharpness of decline, as shown in Fig. 3. For loose sand, since there is no post-peak behavior, $\varphi'_{mob} = \varphi'_{crit}$ and $\psi_{mob} = 0$.

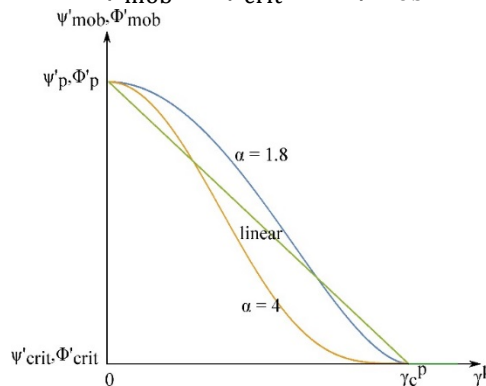


Figure 3. Variation of friction and dilation angle versus plastic shear strain

The soil strength parameters measured from direct shear (DS) test are peak friction angle φ'_{ds-p} , peak dilation angle ψ_p and large-displacement friction angle φ'_{ds-ld} . These parameters were converted to oblique plane strain condition to describe the stress obliquity in the soil, φ'_{ps-p} and φ'_{crit} . The values of φ'_{ds-p} of Cornell University (CU) filter sand were obtained via DS tests by Trautmann and O'Rourke (1985). Olson (2009) conducted DS tests for dry well graded sand, deriving nonlinear regression equation illustrating the decrease of dilation angle with increasing confining stress

$$\frac{\psi_p}{\psi_{p-\sigma'_{Nref}}} = \exp(-0.15 \ln \sigma'_N + 0.08) \quad (6)$$

Davis (1968) derived a relation to calculate φ'_{ps-p}

$$\sin \varphi'_{ps-p} = \frac{\tan \varphi'_{ds-p}}{\cos \psi_p + \sin \psi_p \tan \varphi'_{ds-p}} \quad (7)$$

The modal parameter φ'_{ps-p} is determined as follows: from ratio H/D calculate σ'_N ; then calculate ψ_p from (6) and calculate φ'_{ps-p} from (7). φ'_{crit} is taken from Olson (2009).

Table 1. Input parameters for soils

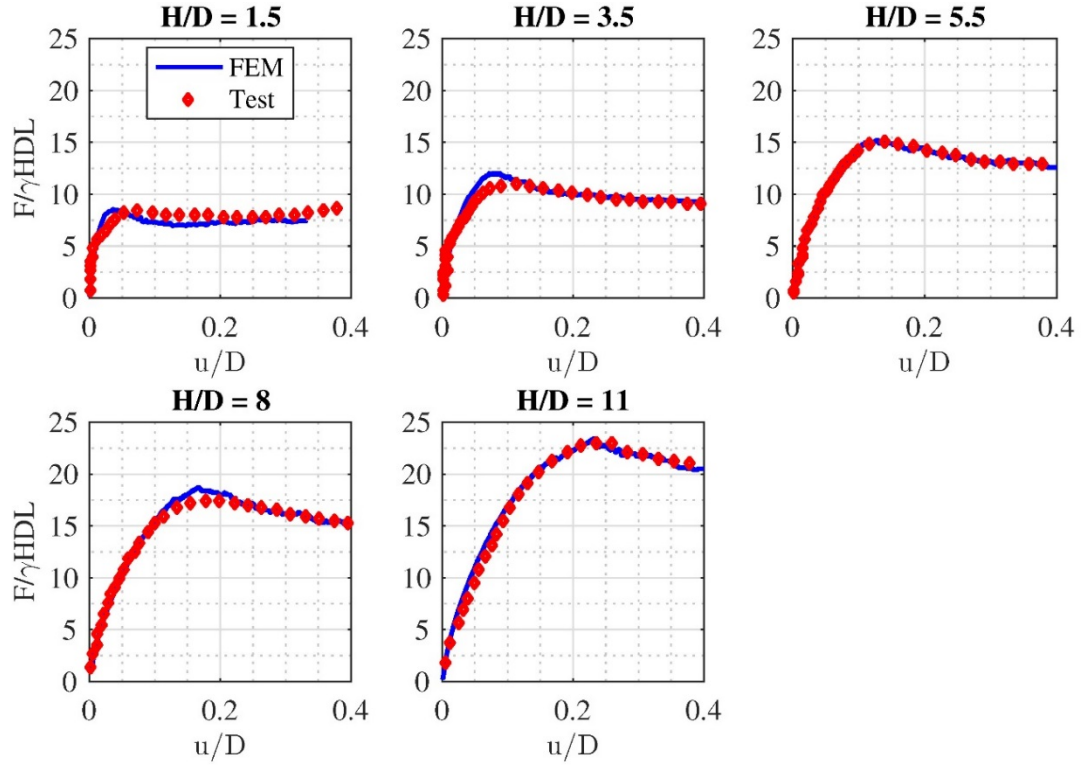
Density	γ (kN/m ³)	Dr (%)	H/D	ψ_p	φ'_{ps-p}	φ'_{crit}
Dense	17.7	80	1.5-11.0	17.5-13.0	49.0-52.0	38.6
Loose	14.8	0	1.5-11.0	0	-	38.6

Parametric studies had been conducted, showing Poisson ratio has negligible effect on the maximum lateral force (less than 5%). Poisson ratio was taken as 0.4 and 0.3 for dense and loose sand. Young modulus E is dependent on mean stress p' followed the equation by Janbu (1963):

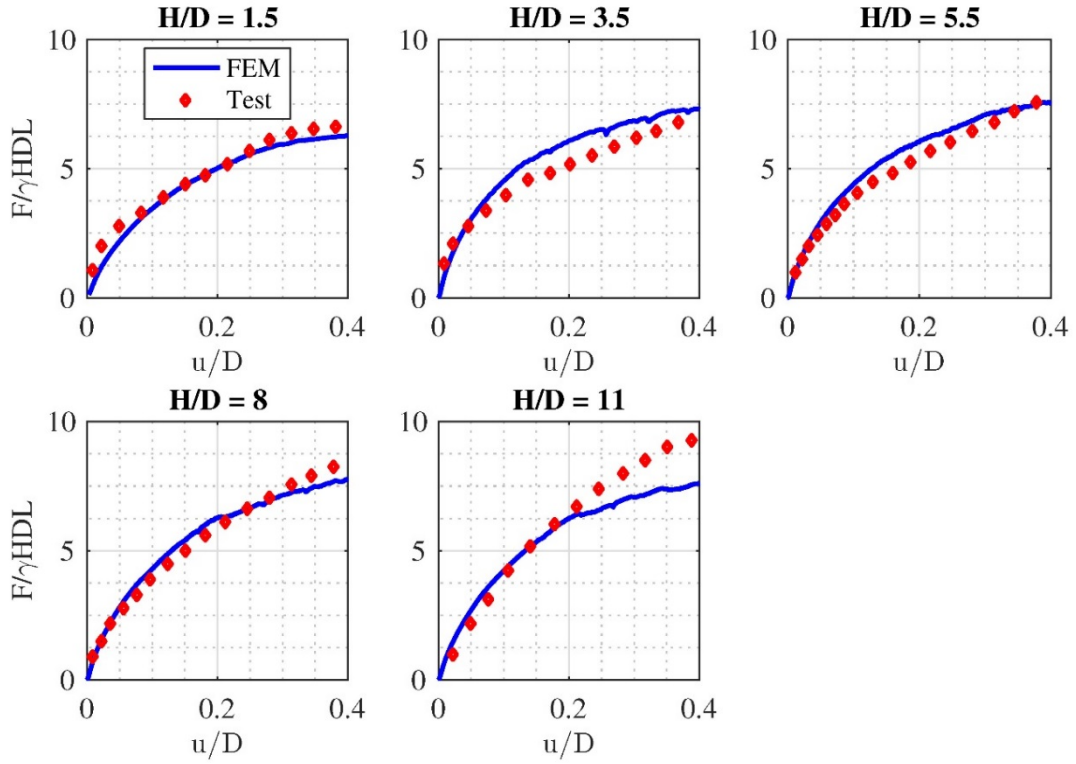
$$E = K_0 p_a \left(\frac{p'}{p_a} \right)^{n_0} \quad (8)$$

Guo and Stolle (2005), Jung et al. (2013), Roy et al. (2015), and Jung et al. (2016) used Eq. 8 to calculate Young modulus at the depth of pipe centerline and assumed it to be constant across the soil domain. Young modulus of soil affects significantly the yield displacement and the smoothness of the transition zone of F - u curve. In this paper, E was calculated at the depth of pipe centerline and it decreased linearly when moving up to the soil surface.

Results validation. The FE results are compared with the tests conducted by Trautmann and O'Rourke (1985) to validate the accuracy of the analyses. The comparison was performed for five different cases of H/D = 1.5, 3.5, 5.5, 8, 11 where H, D is the burial depth and diameter of pipe. Fig. 4 shows the dimensionless lateral reaction $F/(\gamma_s H D L)$ versus the dimensionless lateral displacement u/D from the numerical analyses and the tests. There is a good agreement in both dense and loose sand, proving the fidelity of the numerical simulation. More cases of H/D = 2.5, 4.5, 6, 7, 9, 10 were run afterwards to generate different backbone curves F - u.



(a) Dense sand



(b) Loose sand

Figure 4. Comparison of F-u curves by FE models with Trautmann and O'Rourke tests

THE UNSCENTED KALMAN FILTER

The parameter κ was back-calculated from the F-u curves generated by the FE analyses, using the UKF. This filter is a widely applied state estimation algorithm for nonlinear systems. By using unscented transformation, mean and covariance of state vector are approximated correctly up to the third order (Simon, 2006). From Eq. 1 and 3, the discrete-time nonlinear system for estimating κ is given by

$$\begin{cases} \zeta_{n+1} = \zeta_n + \frac{K}{F_u} \left(1 - \frac{\tanh(\kappa_n |\zeta_n|)}{\tanh \kappa_n} (\beta \text{sign}(\dot{u}_n \zeta_n) + \gamma) \right) (u_{n+1} - u_n) + w_n \\ \kappa_{n+1} = \kappa_n + w'_n \\ F_n = (1 - \alpha) F_u \zeta_n + \alpha K u_n + v_n \end{cases} \quad (9)$$

where the subscript $n, n + 1$ indicate the state parameters at time step t_n, t_{n+1} , respectively; w_n and w'_n are process noise; and v_n is measurement noise.

The results of the UKF are shown in Fig. 5 for the case $H/D = 11$. Analogous procedure was applied to the curves of different H/D cases to generate the variation of κ with pipe burial depth. Fig. 6 shows that κ of loose sand is larger compared to that of dense sand. This is because the transition zone of F - u curve in case of pipe-loose sand interaction is longer and smoother. As shown in Fig. 4a, the reaction force reaches the ultimate value at displacement $u/D = 0.05 - 0.25$ for dense sand. Meanwhile, Fig. 4b shows that the reaction force has not yet reached its ultimate value even until $u/D = 0.4$. Fig. 6 indicates that κ increases as H/D increases from 1.0 to around 5.5, and levels off when $H/D > 5.5$. This trend is likely the same for both loose and dense sand, although the rate of change is much smaller in dense sand. For practical purpose, κ can be chosen as a constant for dense sand. The trend of κ has a lot to do with the failure mechanism of pipe-soil interaction. For shallow burial condition, the soil failure due to large pipe displacement follows the “passive-wedge” mode (Fig. 7). There is an abrupt change from initial linear region to final linear region (yield region) in F - u curve, results in small κ . As the burial depth of pipe increases, the transition zone gradually becomes smoother, κ increases and the soil failure turns into “plow-through” mode (Fig. 8). After the burial depth generating “plow-through” failure mode is reached, κ keeps approximately constant.

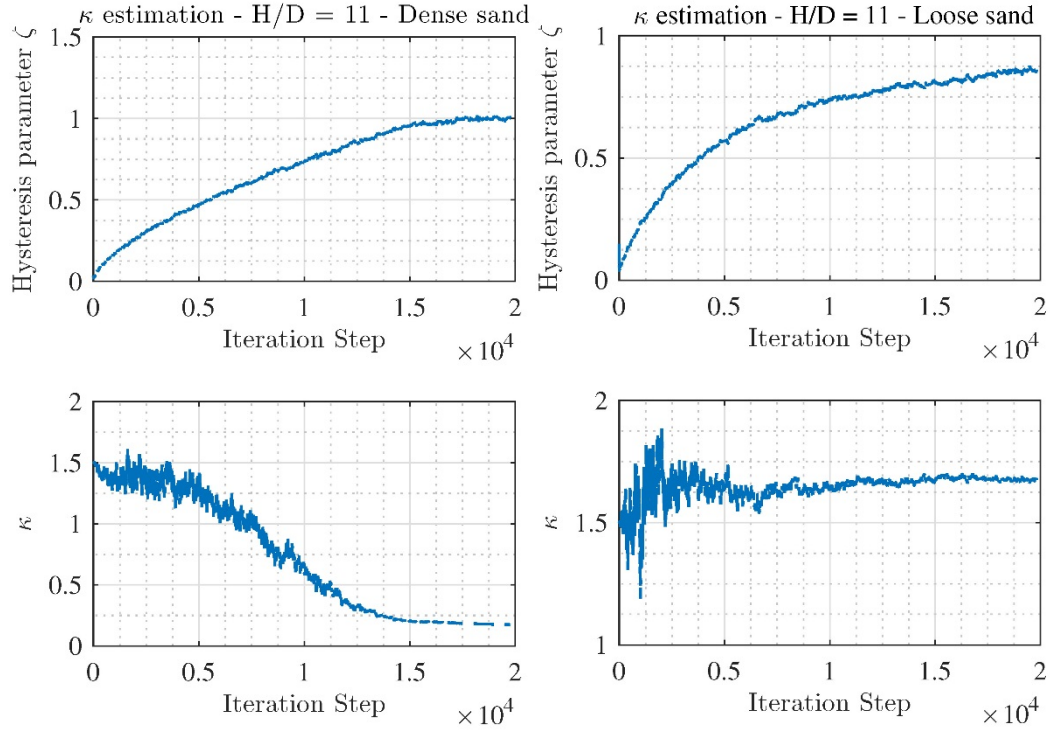


Figure 5. κ estimation from F-u curves for dense and loose sand

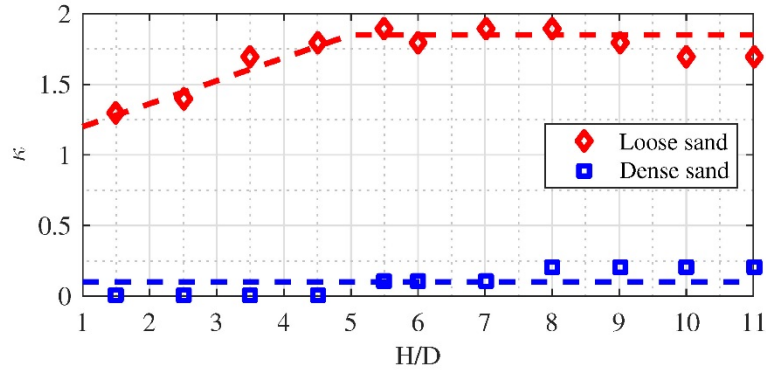


Figure 6. Variation of κ with depth

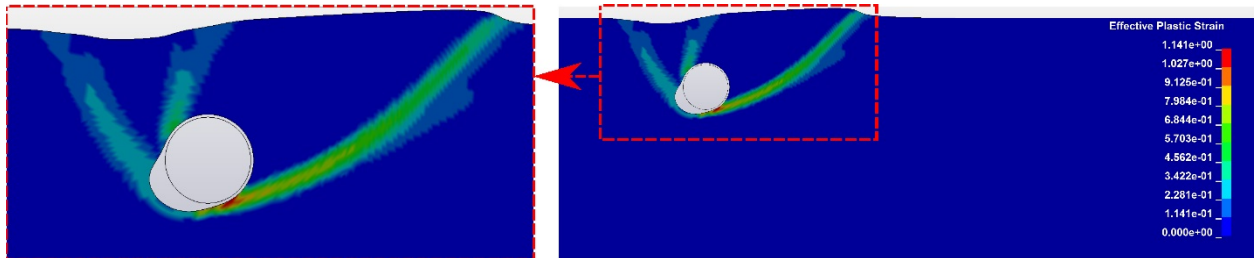


Figure 7. "Passive-wedge" failure mode at $H/D = 1.5$

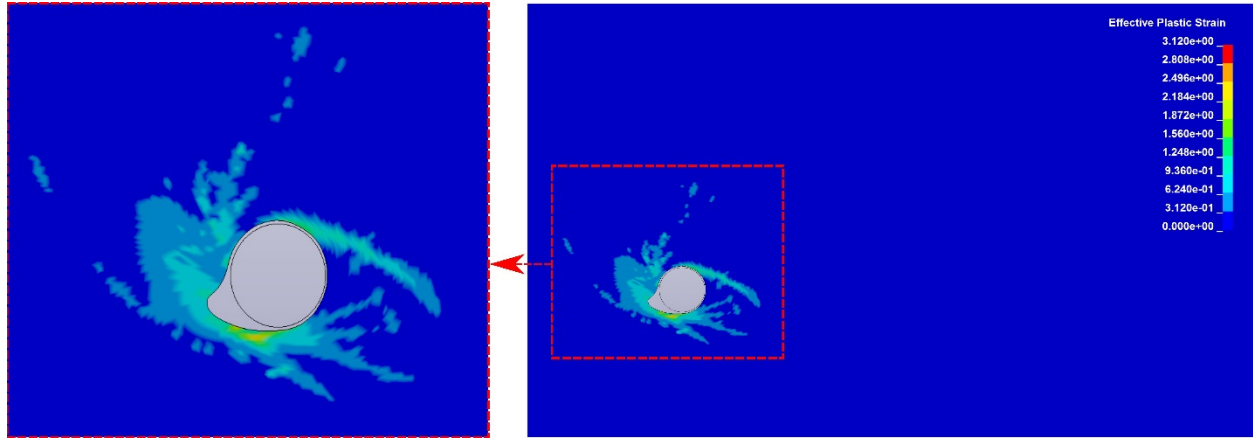


Figure 8. “Plow-through” failure mode at $H/D = 11$

MODIFIED UNIAXIAL BOUC-WEN MODEL VALIDATION

To test the methodology, the $F - u$ curves generated by Eq. 1 and 3 were compared with three different experiments conducted by Audibert and Nyman (1977); Hsu et al. (2001); Karimian et al. (2006). The $F - u$ curves calculated by elasto-plastic (bilinear) model as guided in many guidelines and papers (Trautmann and O’Rourke, 1985; ASCE, 1984; ALA, 2005; PRCI, 2009; Jung et al., 2016) were also presented for comparison. For three critical model parameters, F_u and K were chosen as described in the aforementioned section, κ was taken as in Fig. 6 depending on H/D and type of sand. The input parameters are listed in Table 1. The value $\alpha = 0$, $\beta = 0.5$, $\gamma = 0.5$ were chosen for all three cases.

Table 2. Input parameters for MBW model

Case	H/D	Density	F_u (kN)	K (kN/m)	κ
Audibert and Nyman (1977)	1.5-12.5	Loose	0.11-2.18	220-1550	1.4-1.8
	1.5-12.5	Dense	0.23-4.61	1040-3100	0.1
Hsu et al. (2001)	1.0	Loose	3.18	200	1.2
Karimian et al. (2006)	1.92	Dense	51.32	5570	0.1

The calculated $F - u$ curves from MBW, BW, bi-linear model and experiment data are presented in Fig. 9. The original BW model produces much stiffer behavior in the transition zone in cases of loose sand because the limited range of curvature. Meanwhile, the MBW captures favorably the transition zone of backbone curves. In cases of dense sand, with small κ , the MBW model produces similar results to the original BW model, showing good agreement with the experiment data. Also, the MBW model captures better the $F - u$ curves in the transition zones compared to bilinear approach.

However, in cases of dense sand, the MBW is only capable of representing the $F - u$ curves until the ultimate soil reaction is reached. This is because the methodology is developed based on original BW method which is incapable of describing the post-peak softening behavior.

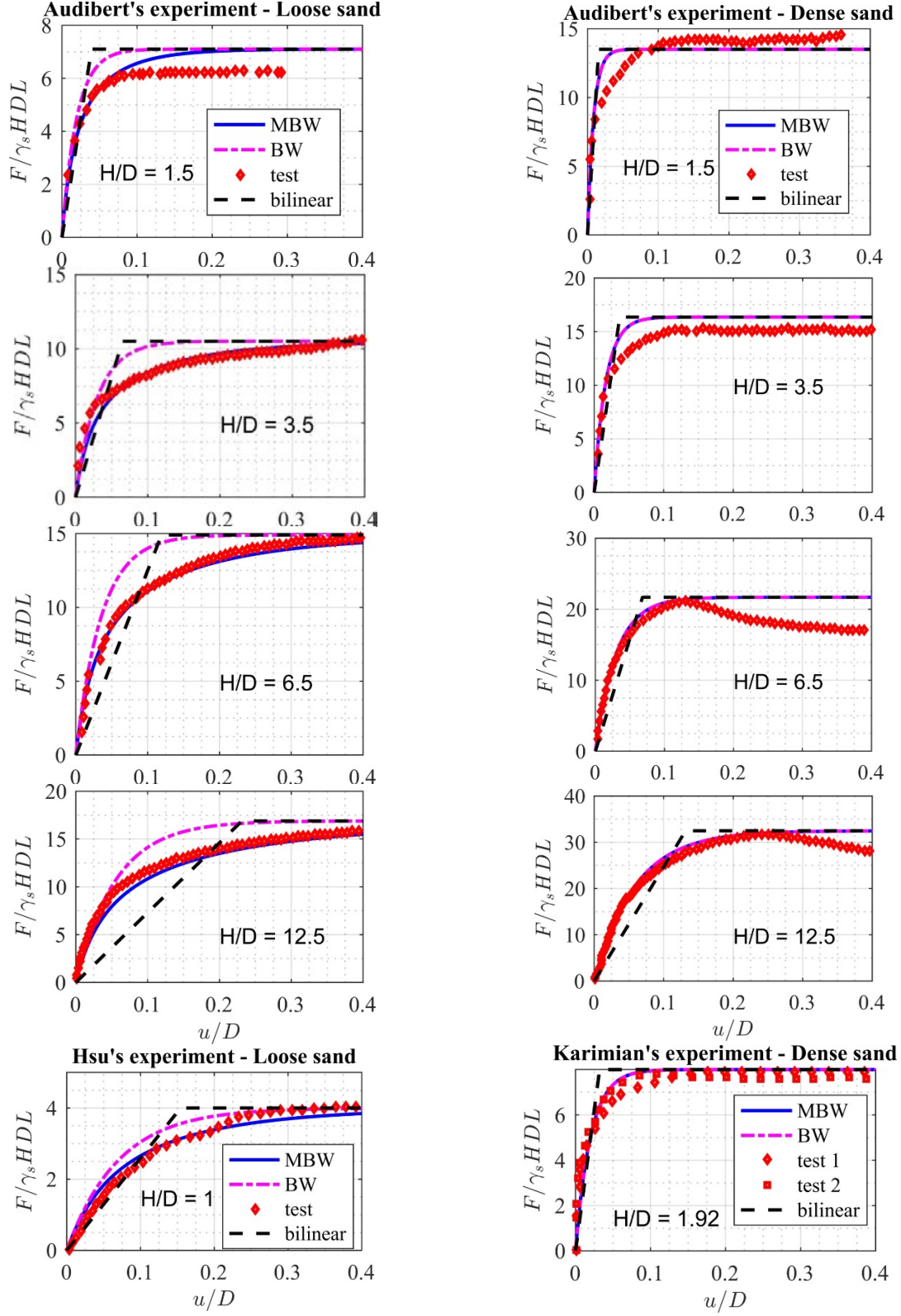


Figure 9. Comparison between MBW, BW ($n=1$), experiments and bilinear model

CONCLUSION

To sum up, our work in this paper based on the results from FE analyses and UKF algorithm to derive parameter κ of loose and dense sand for MBW model. The comprehensive FE model incorporated the post-peak behavior of dense sand by using smooth symmetric beta distribution density function to represent φ'_{mob} and ψ_{mob} gradually decrease to φ'_{crit} and ψ_{crit} . Based on the validated FE models, the backbone curves F - u were generated for different cases of H/D for loose and dense sand. From those curves, UKF was used subsequently to derive κ for the MBW model. The results calculated by MBW model were compared with the experimental data and found to be in good agreement. Some specific findings of interest are

- κ of loose sand, $\kappa = 1.2 - 1.9$, is larger than that of dense sand, $\kappa = 0.0 - 0.2$.
- In the region of “passive-wedge” failure mode, κ increases as the depth H/D increases. In the region of “plow-through” mode, κ approximately levels off.
- For the case of dense sand, while comprehensive FE model is capable of simulating the softening behavior in post-peak region of backbone curves F - u, MBW model is incapable of simulating that behavior.

This study is the first step towards building up a biaxial MBW model to incorporate the coupled behavior of soil springs. Our work also has the potential to be a tool for investigating the cyclic/dynamic pipe-soil interaction.

REFERENCES

- ALA. (2005). Seismic Guidelines for Water Pipelines.
- Anastasopoulos, I., Gazetas, G., Bransby, M. F., Davies, M. C., & El Nahas, A. (2007). Fault rupture propagation through sand: finite-element analysis and validation through centrifuge experiments. *Journal of Geotechnical and Geoenvironmental Engineering*, 133, 943-958.
- ASCE. (1984). Guidelines for the Seismic Design of Oil and Gas Pipeline Systems.
- Audibert, J. M., & Nyman, K. J. (1977). Soil restraint against horizontal motion of pipes. *Journal of the Geotechnical Engineering Division*, 103, 1119-1142.
- Badoni, D., & Makris, N. (1996). Nonlinear response of single piles under lateral inertial and seismic loads. *Soil Dynamics and Earthquake Engineering*, 15, 29-43.
- Bouc, R. (1971). Modele mathematique d'hysteresis. *Acustica*, 21, 16-25.
- Davis, E. H. (1968). Theories of plasticity and the failure of soil masses. Chapter 6 in: Lee, K. 1.(ed.) *Soil Mechanics Selected Topics*. Butterworths.
- Gerolymos, N., & Gazetas, G. (2006). Development of Winkler model for static and dynamic response of caisson foundations with soil and interface nonlinearities. *Soil Dynamics and Earthquake Engineering*, 26, 363-376.

- Guo, P. J., & Stolle, D. F. (2005). Lateral Pipe-Soil Interaction in Sand with Reference to Scale Effect. *Journal of Geotechnical and Geoenvironmental Engineering*, 131, 338-349. doi:10.1061/(ASCE)1090-0241(2005)131:3(338)
- Hallquist, J. O. (2006). LS-DYNA Theory Manual.
- Hsu, T. W., Chen, Y. J., & Wu, C. Y. (2001). Soil friction restraint of oblique pipelines in loose sand. *Journal of transportation engineering*, 127, 82-87.
- Janbu, N. (1963). Soil compressibility as determined by oedometer and triaxial tests. *Proceedings of the European conference on soil mechanics and foundation engineering*, 1, pp. 19-25.
- Jung, J. K., O'Rourke, T. D., & Argyrou, C. (2016). Multi-directional force--displacement response of underground pipe in sand. *Canadian Geotechnical Journal*, 53, 1763-1781.
- Jung, J. K., O'Rourke, T. D., & Olson, N. A. (2013). Lateral soil-pipe interaction in dry and partially saturated sand. *Journal of geotechnical and geoenvironmental engineering*, 139, 2028-2036.
- Karimian, H., Wijewickreme, D., & Honegger, D. (2006). Full-scale laboratory testing to assess methods for reduction of soil loads on buried pipes subject to transverse ground movement. *Proc 6th international pipeline conference, Calgary, Canada*.
- Ma, F., Zhang, H., Bockstedte, A., Foliente, G. C., & Paevere, P. (2004). Parameter analysis of the differential model of hysteresis. *Journal of Applied Mechanics*, 71, 342-349.
- Mitchell, J. K., & Soga, K. (2005). *Fundamentals of soil behavior* (3rd ed ed.). New York ; Chichester : Wiley .
- Olson, N. (2009). *Soil performance for large scale soil-pipeline tests*. Ph.D. dissertation, Cornell University, Ithaca, NY.
- O'Rourke, T. D. (2010). Geohazards and large, geographically distributed systems. *Geotechnique*, 60, 505-543.
- Prisco, C. (2012). Cyclic mechanical response of rigid bodies interacting with sand strata. *Mechanical Behaviour of Soils Under Environmentally Induced Cyclic Loads*, 363-398.
- Roy, K., Hawlader, B., Kenny, S., & Moore, I. (2015). Finite element modeling of lateral pipeline--soil interactions in dense sand. *Canadian Geotechnical Journal*, 53, 490-504.
- Simon, D. (2006). *Optimal State Estimation: Kalman, H Infinity, and Nonlinear Approaches*. Wiley-Interscience.
- Trautmann, C. H., & O'Rourke, T. D. (1985). Lateral force-displacement response of buried pipe. *Journal of Geotechnical Engineering*, 111, 1077-1092.
- Varun, & Assimaki, D. (2012). A generalized hysteresis model for biaxial response of pile foundations in sands. *Soil Dynamics and Earthquake Engineering*, 32, 56-70. doi:https://doi.org/10.1016/j.soildyn.2011.08.004
- Varun, Dominic, A., & Abdollah, S. (2013). Soil-pipe-structure interaction simulations in liquefiable soils via dynamic macroelements: Formulation and validation. *Soil Dynamics and Earthquake Engineering*, 47, 92-107. doi:https://doi.org/10.1016/j.soildyn.2012.03.008
- Wen, Y.-K. (1976). Method for random vibration of hysteretic systems. *Journal of the engineering mechanics division*, 102, 249-263.